ANTIOXIDANTS & REDOX SIGNALING
Volume 15, Number 9, 2011

DOI: 10.1089/ars.2010.3825

ORIGINAL RESEARCH COMMUNICATION

Increased Expression of the Transient Receptor Potential Melastatin 7 Channel Is Critically Involved in Lipopolysaccharide-Induced Reactive Oxygen Species-Mediated Neuronal Death

Felipe Nuñez-Villena,[1,*] Alvaro Becerra,[1,*] Cesar Echeverría,[1,*] Nicolás Briceño,[1] Omar Porras,[2] Ricardo Armisén,[2] Diego Varela,[2] Ignacio Montorfano,[1] Daniela Sarmiento,[1] and Felipe Simon[1]

Abstract

Aims: To assess the mechanisms involved in lipopolysaccharide (LPS)-induced neuronal cell death, we examined the cellular consequences of LPS exposure in differentiated PC12 neurons and primary hippocampal neurons. ***Results:*** Our data show that LPS is able to induce PC12 neuronal cell death without the participation of glial cells. Neuronal cell death was mediated by an increase in cellular reactive oxygen species (ROS) levels. Considering the prevalent role of specific ion channels in mediating the deleterious effect of ROS, we assessed their contribution to this process. Neurons exposed to LPS showed a significant intracellular Ca^{2+} overload, and nonselective cationic channel blockers inhibited LPS-induced neuronal death. In particular, we observed that both LPS and hydrogen peroxide exposure strongly increased the expression of the transient receptor protein melastatin 7 (TRPM7), which is an ion channel directly implicated in neuronal cell death. Further, both LPS-induced TRPM7 overexpression and LPS-induced neuronal cell death were decreased with dithiothreitol, diphenyliodonium, and apocynin. Finally, knockdown of TRPM7 expression using small interference RNA technology protected primary hippocampal neurons and differentiated PC12 neurons from the LPS challenge. ***Innovation:*** This is the first report showing that TRPM7 is a key protein involved in neuronal death after LPS challenge. ***Conclusion:*** We conclude that LPS promotes an abnormal ROS-dependent TRPM7 overexpression, which plays a crucial role in pathologic events, thus leading to neuronal dysfunction and death. *Antioxid. Redox Signal*. 15, 2425–2438.

Introduction

Bacterial nervous system infections remain a common cause of human mortality in spite of new drugs and treatment approaches (29). The major determinant of the bacterial cytotoxic effect is a component of the outer membrane in Gram-negative bacteria, lipopolysaccharide (LPS). Interactions between LPS and the nervous system are involved in several neurodegenerative disorders including encephalitis, meningitis, and Parkinson's disease (30, 31, 61). The presence of LPS in capillaries increases vascular permeability, allowing LPS penetration into neuronal territory (34). The subsequent neuroinflammatory response triggered by LPS induces neurodegeneration and neuronal death (11).

Innovation

It is currently accepted that lipopolysaccharide (LPS) induced neurotoxicity is induced through microglia activation. However, LPS-induced neurotoxicity in absence of microglia has not been reported. In this work, we showed that LPS challenge was able to induce neuronal death in absence of microglia throughout the crucial participation of transient receptor potential melastatin 7 (TRPM7) in an ROS-dependent mechanism. In addition, we reported that neurons exposed to LPS showed an ROS-dependent increase of TRPM7 expression. Thus, we envisage that TRPM7 turns in a novel target for drug development in the treatment of Gram-negative bacterial nervous system infections.

[1]Departamento de Ciencias Biologicas, Facultad de Ciencias Biologicas & Facultad de Medicina, Universidad Andres Bello, Santiago, Chile.
[2]Facultad de Medicina, Centro de Estudios Moleculares de la Célula, CEMC, & Instituto de Ciencias Biomédicas, ICBM, Universidad de Chile, Santiago, Chile.
*These authors contributed equally to this work.

Reactive oxygen species (ROS), such as superoxide radical ($O_2^{\bullet -}$), hydrogen peroxide (H_2O_2), and hydroxyl radical ($^{\bullet}OH$), are endogenously produced cellular molecules involved in a broad range of physiologic and pathophysiologic cellular processes, such as regulation of cell proliferation and survival, oncogene activation, apoptosis, and necrosis (32, 33, 38). It has been reported that ROS can regulate gene expression and play a role as a signaling molecule to modulate protein function (10, 24). H_2O_2 and other reactive oxygen intermediates are involved in the expression of a number of proteins, such as vascular cell adhesion molecule-1 (VCAM-1), intercellular adhesion molecule-1 (ICAM-1) (44), the protooncogenes c-jun, c-fos, and c-myc (26), cyclooxygenase-2, and prostaglandins (22). The effects of ROS on gene expression are mainly mediated by activating transcription factors, such as NF-κB, activator protein-1 (AP-1), hypoxia-inducible factor-1 (HIF-1), and the JAK-STAT pathway (12, 47, 50, 55).

Further, exposure to LPS induces an increase in oxidative stress in a number of cell types (18, 41, 51, 53). ROS production promotes a broad range of favorable effects in cellular physiology (10). However, deleterious effects of ROS, including promotion of cellular dysfunction and death, have also been extensively reported. The nervous system seems to be particularly vulnerable to ROS due to its high metabolic rate, deficient anti-oxidant defense mechanisms, and diminished cellular turnover rate (23). During sepsis, it is well accepted that LPS promotes neuronal cell death indirectly by activating microglia, astrocytes, and other immune cells (40). However, recently it has been reported that neurons exposed to LPS exhibit cell death even in the absence of other cell types, suggesting a direct effect of LPS on neuron viability (4, 25, 65). The mechanism involved in LPS-induced neuronal cell death has not yet been established.

The transient receptor potential (TRP) superfamily is a diverse group of nonselective cationic channels (NSCCs) expressed in several mammalian cell types (13, 37, 60). There is a well-documented link between the TRP melastatin-related type 7 cation channel (TRPM7) and oxidative stress-induced neuron injury (35). TRPM7 not only has a nonselective conductance for Ca^{2+} and Mg^{2+} but also has kinase activity (39, 45). Although the participation of TRPM7 has been demonstrated in several physiologic processes, extensive evidence supports the finding that TRPM7 is a critical determinant in oxidative stress-induced cell death, especially in neurons (35). Suppression of TRPM7 expression in primary cortical neurons with RNA interference protects cells from anoxia, suggesting a role for endogenous TRPM7 in anoxic cell death (1). ROS activation and enhancement of cation conductance is likely mediated through TRPM7 (1, 35). Concordantly, overexpression of TRPM7 in human embryonic kidney (HEK) cells results in cell swelling, detachment, and cell death (1, 39). In addition, suppression of TRPM7 in hippocampal neurons leads to neuronal protection during hypoxic-ischemic injury to the brain (56).

In this article, we address the question of whether LPS can induce TRPM7-dependent neuronal cell death in the absence of other cells and explore the cellular consequences of LPS exposure on differentiated PC12 neurons and primary hippocampal neurons. Here, we show that LPS can directly induce neuronal cell death and that this process is mediated by an increase in ROS levels, which result in increased TRPM7 expression.

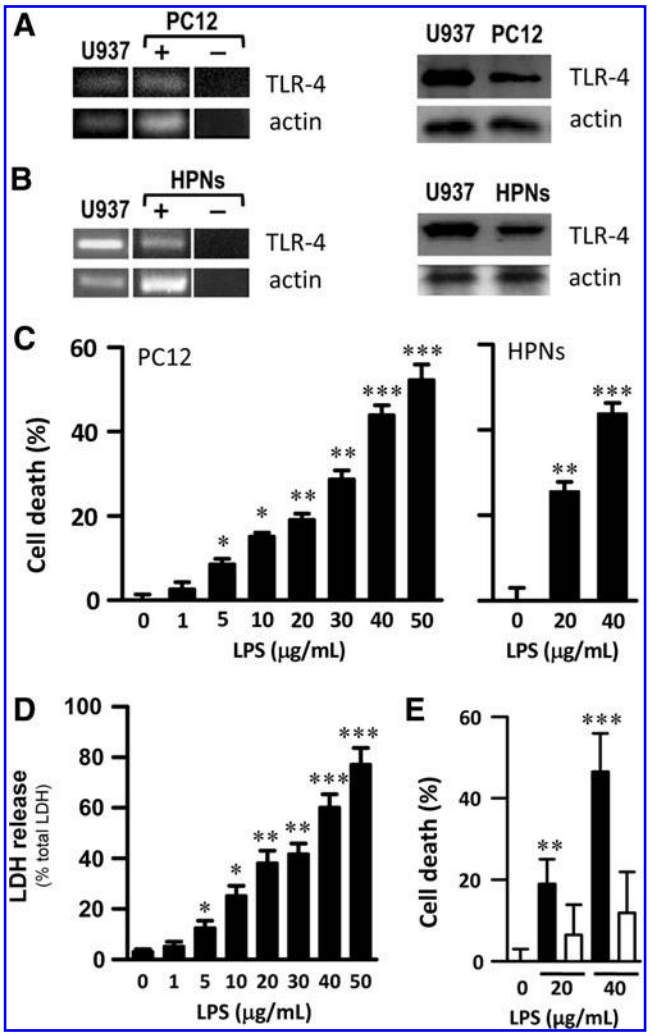

FIG. 1. Lipopolysaccharide (LPS)-induced neuronal cell death. mRNA (*left panel*) and protein (*right panel*) detection of TLR-4 by retrotranscriptase–polymerase chain reaction (RT-PCR) and Western blot, respectively, in differentiated PC12 neurons **(A)** or hippocampal primary neurons (HPNs) **(B)**. The U937 cell line was used as a positive control. (+): PC12/HPNs samples; (−): non-RT sample. Actin was used as a loading control. **(C)** Changes in neuronal death determined by MTT assay in differentiated PC12 neurons exposed to 0, 1, 5, 10, 20, 30, 40, and 50 μg/ml LPS (*left panel*) or HPNs exposed to 0, 20, and 40 μg/ml LPS (*right panel*) for 48 h. **(D)** Lactate dehydrogenase (LDH) release of differentiated PC12 neurons exposed to 0, 1, 5, 10, 20, 30, 40, and 50 μg/ml LPS for 48 h. **(E)** Effect of TBX2 on LPS-induced neuronal death. Differentiated PC12 neurons were exposed to 0, 20, and 40 μg/ml LPS in the presence (empty bars) or absence (filled bars) of 160 μM TBX2. Statistical differences were assessed by one-way ANOVA (Kruskal–Wallis) followed by Dunns *post hoc* test. $^*p<0.05$, $^{**}p<0.01$, and $^{***}p<0.001$ compared with 0 μg/ml LPS. Graph bars show the mean ± SD. ($n=5$–7).

Results

LPS activates ROS production and cell death

To study the impact of LPS on neuronal cell death, we utilized nerve growth factor (NGF)-differentiated PC12 neuronal cells. Since it is a matter of debate whether neurons

directly respond to LPS, first we examined LPS receptor expression in this pure population of neurons. Toll-like receptor-4 (TLR-4) expression has been reported in various neuronal cell types, such as cultured myenteric neurons from rat small intestine (4), primary mouse cortical neurons (57), human neuronal-like cell line NTera2 (43), mouse neurons *in vivo* (36), rat trigeminal sensory neurons (62), and mouse cortical neurons (58). However, to our knowledge, no TLR-4 expression in differentiated PC12 cells has been previously demonstrated. As shown in Figure 1A, differentiated PC12 neurons expressed TLR-4 at both the mRNA (Fig. 1A, left panel) and protein levels (Fig. 1A, right panel), whereas undifferentiated PC12 neurons did not (data not shown). Concordantly, TLR-4 expression was detected in rat hippocampal primary neurons (HPNs) at mRNA (Fig. 1B, left panel) and protein levels (Fig. 1B, right panel).

To test the effect of LPS, differentiated PC12 neurons and HPNs were exposed to different doses of LPS for 48 h, and cell death was measured by MTT reduction assay. The exposure of differentiated PC12 neurons to a dose of LPS as low as 5 μg/ml led to enhanced cell death, and a clear dose-response relationship was observed when higher doses were used (up to 50 μg/ml, Fig. 1C, left panel). Similarly, HPNs exposed to LPS showed a dose-response cell death similar to the one observed in PC12 neurons in the same concentration range (Fig. 1C, right panel). Accordingly, the lactate dehydrogenase (LDH) release assay showed a dose-dependent LPS-induced PC12 differentiated neuron death (Fig. 1D), confirming the results observed with MTT reduction assay.

To demonstrate that the neurotoxic effect of LPS occurred through TLR-4, we performed an experiment using the specific TLR-4 signaling inhibitor TBX2 (28). Differentiated PC12 neurons exposed to LPS and cultured in the presence of TBX2 were significantly resistant to the LPS challenge. This result suggests that the neurotoxicity of LPS is mediated through TLR-4 (Fig. 1E).

To further explore the mechanisms underlying LPS-induced cell death of differentiated PC12 neurons, we measured ROS production in these cells. Since TLR-4 activation leads to an increase of NAD(P)H oxidase activity, we reasoned that LPS may increase cellular ROS levels. Indeed, previous work had shown that the intracellular ROS source, NAD(P)H oxidase, could be involved in LPS-induced ROS-mediated cell death in other cell types (7, 8, 25, 51). Differentiated PC12 neurons were exposed to 20 μg/ml LPS for 48 h, and ROS cellular levels were evaluated with two different ROS-sensitive fluorescent probes using flow cytometry. Control cells exhibited a uniform staining with the ROS-sensitive dye dichlorodihydrofluorescein (DCF) (Fig. 2A). In contrast, LPS-exposed cells show a significant increase in the proportion of cells displaying high levels of DCF fluorescence (Fig. 2B). Similar results were obtained with diacetate dihydroethidium (DHE), a probe used to detect superoxide anions. LPS exposure significantly increases the proportion of cells with

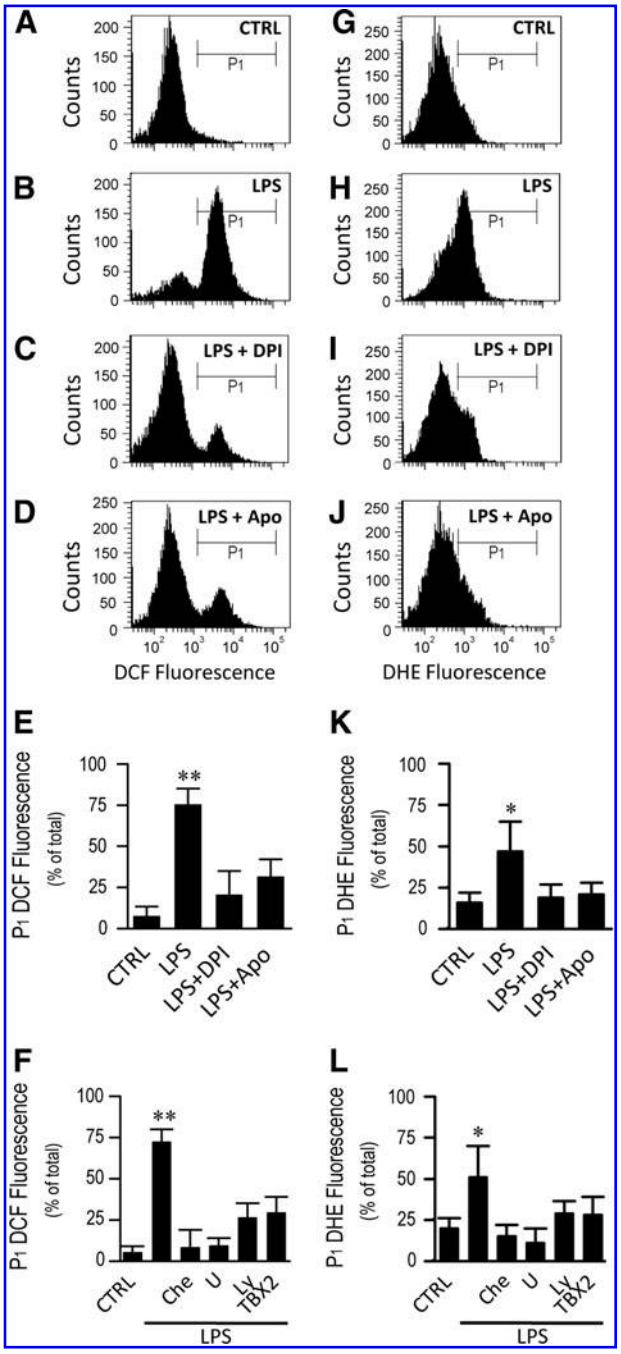

FIG. 2. LPS-induced NAD(P)H oxidase-dependent neuronal reactive oxygen species (ROS) production. Representative dichlorodihydrofluorescein (DCF) **(A–D)** and diacetate dihydroethidium (DHE) **(G–J)** fluorescence histograms from separate experiments of differentiated PC12 neurons exposed to either vehicle alone **(A** and **G)**, 20 μg/ml LPS **(B** and **H)**, 20 μg/ml LPS with 2 μM diphenyleneiodonium sulfate (DPI) **(C** and **I)**, or 20 μg/ml LPS with 1 mM Apocynin (Apo) **(D** and **J)** for 48 h. Data obtained from several experiments, including those depicted in the histograms above, are summarized in **(E** and **K)** for DCF and DHE, respectively. Differentiated PC12 neurons exposed to either vehicle alone, 20 μg/ml LPS, 20 μg/ml LPS with 1 μM Chelerythrine (Che), 20 μg/ml LPS with 1 μM U73122 (U), 20 μg/ml LPS with 1 mM Ly294002 (Ly) or 20 μg/ml LPS with 160 μM TBX2 for 48 h, and DCF **(F)** or DHF **(L)** fluorescence was measured. Graphs show the percentage (mean ± SD) of cells within the P_1 population of DCF or DHE fluorescence. Statistical differences were assessed by one-way ANOVA (Kruskal–Wallis) followed by Dunns *post hoc* test. *$p < 0.05$; **$p < 0.01$ relative to 0 μg/ml LPS.

elevated DHE fluorescence (Fig. 2G, H). These results suggest that the overall increase in ROS cellular levels, measured with DCF, is due to an increase in anion superoxide levels.

To explore the source of ROS production, we exposed PC12 cells to LPS in the presence of diphenyleneiodonium sulfate (DPI) and Apocynin (Apo) (17, 19, 42, 64), which are non-specific NAD(P)H oxidase inhibitors, and measured cellular levels of ROS. As depicted in Figure 2C and 2I, DPI significantly prevented an increase in ROS production in both DCF and DHE assays. Similar results were obtained using Apo (Fig. 2D, J). Experiments shown in Figure 2A–D and 2G–J, which were performed with DCF and DHE, respectively, are summarized in Figure 2E and 2K.

Considering that protein kinase C (PKC) is critically involved in NAD(P)H oxidase activation (27) and that phospholipase C (PLC) and phosphoinositide 3-kinase (PI3-K) are involved in PKC activation, we addressed whether they played a role in LPS-induced ROS production. Therefore, we used the generic PKC inhibitor, Chelerythrine (Che), the PLC inhibitor, U73122 (U), and the generic inhibitor of PI3-K, Ly294002 (Ly). Further, to examine whether LPS-induced ROS production occurred through TLR-4, we performed experiments with TBX2. LPS-induced ROS production was decreased when differentiated PC12 cells were cultured simultaneously with LPS and Che, U, Ly, or TBX2 (Fig. 2F, L, using DCF and DHE, respectively).

An increase in ROS cellular levels may explain the increase in cell death observed after neuron exposure to LPS. To explore the participation of ROS in the cell death process, we performed the LPS exposure experiments in the presence of the strong reducing agent dithiothreitol (DTT). As illustrated in Figure 3A, increasing doses of DTT significantly inhibited the increase in neuronal death observed after LPS exposure in differentiated PC12 neurons (Fig. 3A, left panel) and HPNs (Fig. 3A, right panel).

To confirm that ROS are capable of compromising cell viability in this cell model, PC12 neurons were exposed to a range of H_2O_2 concentrations. H_2O_2 is produced in cells after superoxide dismutase reacts with anion superoxide. As shown in Figure 3B, H_2O_2 concentrations as low as 1 μM induced a significant increase in neuronal cell death. These results are consistent with data obtained by Coombes *et al.* (9) in primary neuronal cultures.

To explore whether LPS-induced NAD(P)H oxidase activation participates in the observed increase in cell death, LPS exposure experiments were performed in the presence of DPI and Apo. DPI and Apo significantly inhibited the increase in neuronal death observed after LPS exposure in differentiated PC12 neurons (Fig. 3C, left panel) and HPNs (Fig. 3C, right panel). Also, neuronal cell death was reduced by culturing LPS-induced differentiated PC12 cells simultaneously with Chelerythrine, U73122, or Ly294002 (Fig. 3D). Overall, our results suggest that LPS activates NAD(P)H oxidase, which, in turns, increases ROS production, resulting in neuronal cell death.

Role of NSCCs in LPS-induced PC12 neuron cell death

Alterations in intracellular calcium levels can modulate cell death in almost all cell types. These calcium fluxes are determined by the activity of membrane ion channels and are regulated through several mechanisms. It is increasingly

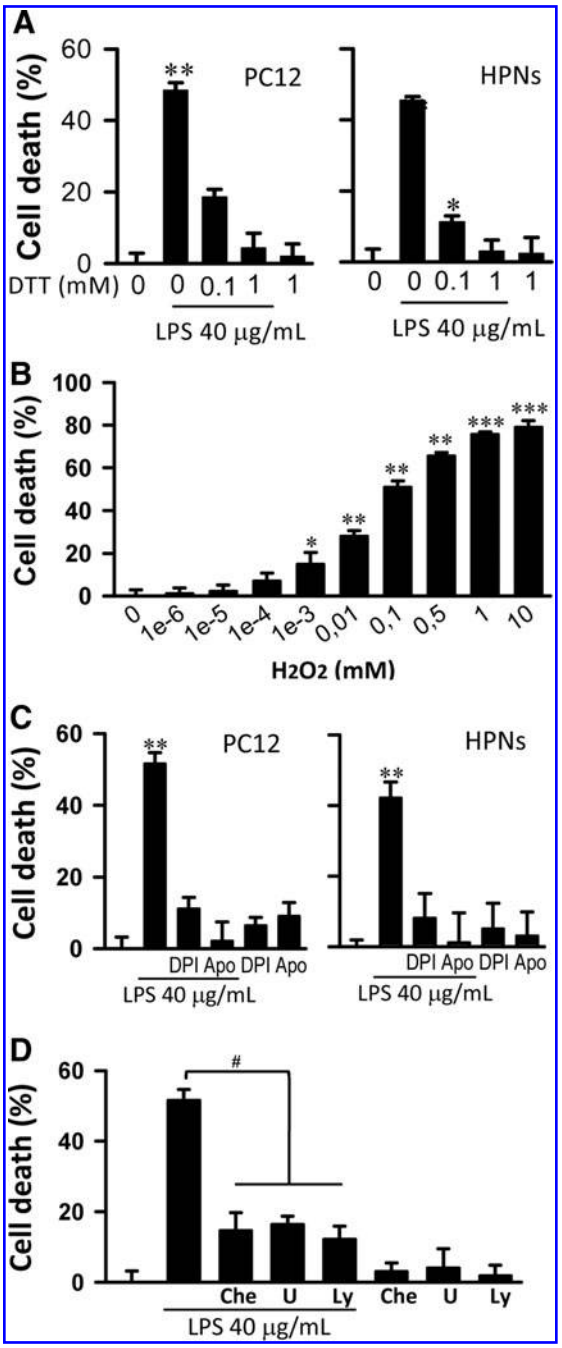

FIG. 3. LPS-induced ROS-mediated neuronal cell death. **(A)** Changes in cell death of differentiated PC12 neurons (*left panel*) and HPNs (*right panel*) exposed to 40 μg/ml LPS for 48 h in the presence or absence of DTT. **(B)** Changes in cell death of differentiated PC12 neurons exposed to different hydrogen peroxide (H_2O_2) concentrations in the absence of LPS for 48 h. **(C)** Changes in cell death of differentiated PC12 neurons (*left panel*) and HPNs (*right panel*) exposed to 40 μg/ml LPS for 48 h in the presence of 2 μM DPI (DPI) and 1 mM Apo. **(D)** Changes in cell death of differentiated PC12 neurons exposed to 40 μg/ml LPS for 48 h in the presence of 1 μM Chelerythrine (Che), 1 μM U73122 (U), or 1 μM Ly294002 (Ly). Statistical differences were assessed by one-way ANOVA (Kruskal–Wallis) followed by Dunns *post hoc* test. * $p < 0.05$, ** $p < 0.01$, and *** $p < 0.01$ against 0 μg/ml LPS. # $p < 0.05$ against 40 μg/ml LPS. Graph bars show the mean ± SD ($n = 9$–12).

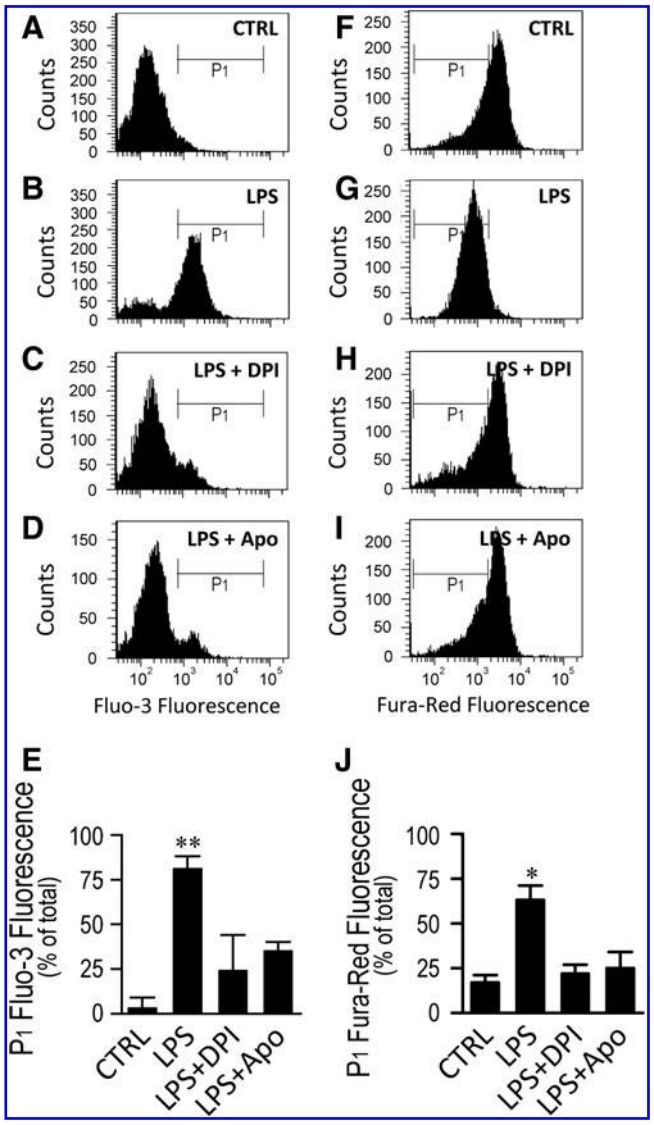

FIG. 4. LPS-induced Ca^{2+} overload in neurons. Representative Fluo-3 **(A–D)** and Fura-Red **(F–I)** fluorescence histograms from separate experiments of differentiated PC12 neurons exposed to either vehicle alone **(A** and **F)**, 20 μg/ml LPS **(B** and **G)**, 20 μg/ml LPS with 2 μM DPI **(C** and **H)**, or 20 μg/ml LPS with 1 mM Apo **(D** and **I)** for 48 h. Data obtained from experiments as those depicted in the histograms above were summarized **(E, J)**. Graph bars show the percentage (mean ± SD) of cells within the P_1 population of Fluo-3 **(E)** or Fura-Red **(J)** fluorescence. ($N = 4$). Statistical differences were assessed by one-way ANOVA (Kruskal–Wallis) followed by Dunns *post hoc* test. $^*p < 0.05$ and $^{**}p < 0.01$ against 0 μg/ml LPS.

apparent that many ion channels are affected by ROS (3, 15, 46). Therefore, we explored whether the ROS increase observed after LPS exposure may interfere with cellular calcium homeostasis. Considering that cell death is often accompanied by changes in cellular volume, intracellular calcium levels were measured independently with two different calcium-sensitive fluorescent probes, one that increases (Fluo-3) and another that decreases (Fura-Red) in fluorescence on calcium binding. Differentiated PC12 neurons were exposed to 20 μg/ml of LPS for 48 h, and intracellular calcium levels were measured using the calcium-sensitive probes and flow cytometry. LPS-exposed cells showed a significant increase in the proportion of cells with higher intracellular calcium as measured with both Fluo-3 and Fura-Red (Fig. 4A, B and F, G), indicating that the changes in fluorescence are not related to concomitant changes in cell volume. To determine whether LPS-induced ROS generation was involved in calcium influx, we performed experiments using DPI and Apo. As depicted in Figure 4C and 4H, DPI significantly prevented an increase in intracellular calcium. Similar results were obtained using Apo (Fig. 4D, I). Several experiments, as shown in Figure 4A–D and 4F–I, conducted with Fluo-3 and Fura-Red, respectively, are summarized in Figure 4E and 4J.

Previous work has shown that a number of NSCCs could be involved in intracellular calcium deregulation (15). In neurons, compelling evidence shows that TRPM7 activity increases in response to ROS and results in neuronal cell death (1, 9) in the context of brain ischemia. Due to the lack of specific pharmacological inhibitors, first we assessed the effect of polyvalent cations that inhibit a range of NSCCs, including TRPM7 channels (1, 20). Gd^{3+} or Zn^{2+} blocked LPS-induced cell death in a dose-response manner in differentiated PC12 neurons and in HPNs (Fig. 5), suggesting the participation of NSCCs such as TRPM7 in this process.

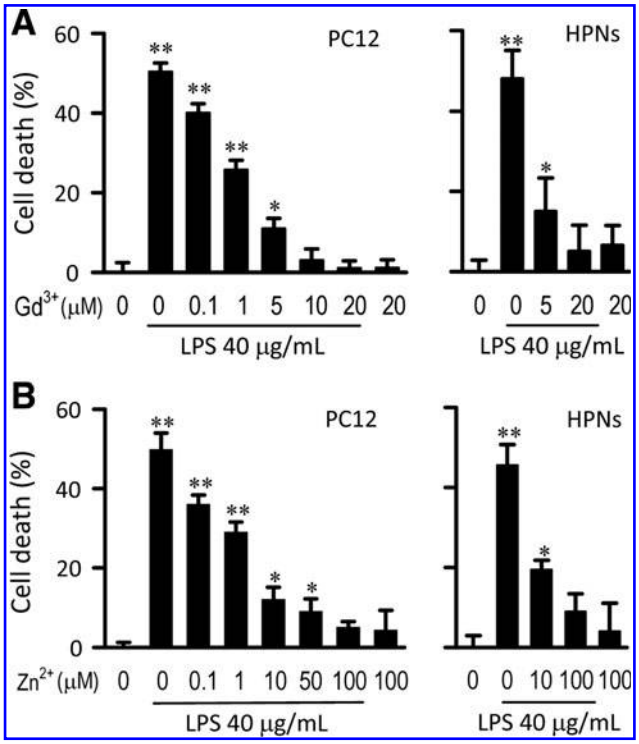

FIG. 5. LPS-induced neuronal cell death is abolished with cationic channels inhibitors. Changes in cell death of differentiated PC12 neurons (*left panel*) and HPNs (*right panel*) exposed to 40 μg/ml LPS for 48 h in the presence of different Gd^{3+} **(A)** and Zn^{2+} **(B)** concentrations. Statistical differences were assessed by one-way ANOVA (Kruskal–Wallis) followed by Dunns *post hoc* test. $^*p < 0.05$ and $^{**}p < 0.01$ against 0 μg/ml LPS. Graph bars show the mean ± SD ($n = 4$).

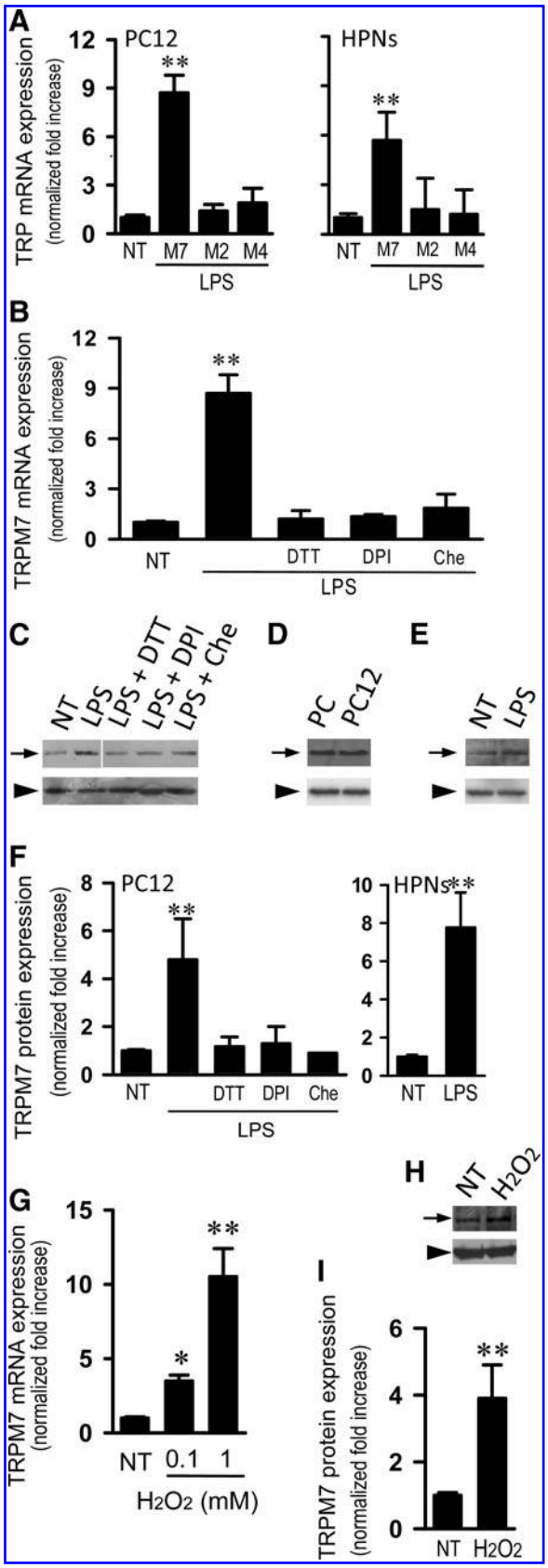

LPS and ROS induce an increase in TRPM7 mRNA and protein expression in PC12 neurons

Previous work has shown that NSCCs activity is modulated by ROS (15, 52, 54, 59); however, since the identification of some of the genes encoding NSCCs, it has been suggested that their expression could also be modulated by ROS (21, 48, 49, 63). To explore this possibility, we measured TRPM2, TRPM4, and TRPM7 mRNA using quantitative polymerase chain reaction (qPCR) in differentiated PC12 neurons and HPNs exposed to LPS. As shown in Figure 6A, a significant ~8-fold and ~6-fold increase in TRPM7 mRNA expression was observed in differentiated PC12 neurons and HPNs, respectively, whereas no changes were seen in the other genes. The LPS-induced TRPM7 mRNA expression increase was inhibited by DTT, DPI, and Chelerythrine (Fig. 6B). As shown in Figure 6C, the LPS-induced increase in TRPM7 mRNA was paralleled by an increase in TRPM7 protein in differentiated PC12 neurons (Fig. 6C) and in HPNs (Fig. 6E). As a control for the TRPM7 antibody specificity, HEK293 cells were transfected with a plasmid encoding the TRPM7 cDNA. As shown in Figure 6D, a band of similar size was detected in differentiated PC12 neurons and in HEK293 cells transfected with TRPM7 cDNA (Fig. 6D). The ability of LPS to increase TRPM7 protein levels was inhibited by DTT, DPI, and Chelerythrine (Fig. 6C, F). To confirm that ROS are able to modulate TRPM7 expression, differentiated PC12 neurons were exposed to low doses of H_2O_2 for 48 h. H_2O_2 exposure induced a significant increase in TRPM7 mRNA and protein (Fig. 6H–I).

FIG. 6. LPS- and H_2O_2-induced increase of transient receptor potential melastatin 7 (TRPM7) expression. (A) Changes in mRNA expression of TRPM7 (M7), TRPM2 (M2), and TRPM4 (M4) in differentiated PC12 neurons (*left panel*) and HPNs (*right panel*) exposed to 20 μg/ml LPS for 48 h. Changes in mRNA expression **(B)** and protein levels **(C)** of TRPM7 in differentiated PC12 neurons exposed to 20 μg/ml LPS for 48 h in the presence of 1 μM DTT (DTT), 2 μM DPI (DPI), and 1 μM Chelerythrine (Che). mRNA expression was normalized relative to nontreated cells (nontransfected [NT]). NT shows a summary of TRPM7, M2, and M4 mRNA expression in nontreated cells. **(D)** Detection of TRPM7 protein in differentiated PC12 neurons (PC12) and in overexpressed TRPM7 protein in HEK cells, as a positive control (PC). **(E)** Changes in protein levels of TRPM7 in HPNs exposed to 20 μg/ml LPS for 48 h **(C–E)**. *Arrows* depict TRPM7. *Arrowheads* indicate tubulin, which was used as loading control. **(F)** Densitometric analyses for separate experiments as shown in C (differentiated PC12 neurons, *left panel*) and E (HPNs, *right panel*) normalized against 0 μg/ml LPS (NT). Proteins levels were calculated relative to tubulin. Changes in mRNA expression **(G)** and protein levels **(H)** of TRPM7 in differentiated PC12 neurons exposed to H_2O_2 for 48 h. mRNA expression was normalized relative to nontreated cells (NT). *Arrows* depict TRPM7. *Arrowheads* indicate tubulin, which was used as loading control. **(I)** Densitometric analyses from separate experiments as shown in **(H)** normalized against 0 μg/ml LPS (NT). Protein levels were measured relative to tubulin. Statistical differences were assessed by one-way ANOVA (Kruskal–Wallis) followed by Dunns *post hoc* test for **(A)**, **(B)**, **(F)** (*left panel*), **(G)**, and Student's *t*-test (Mann–Whitney) for **(F)** (*right panel*) and **(I)**. $*p < 0.05$, $**p < 0.01$ compared with 0 μg/ml LPS (NT). Graphs show the mean ± SD. $n = 4$–8 for **(A–F)** and $n = 3$–4 for **(G–I)**.

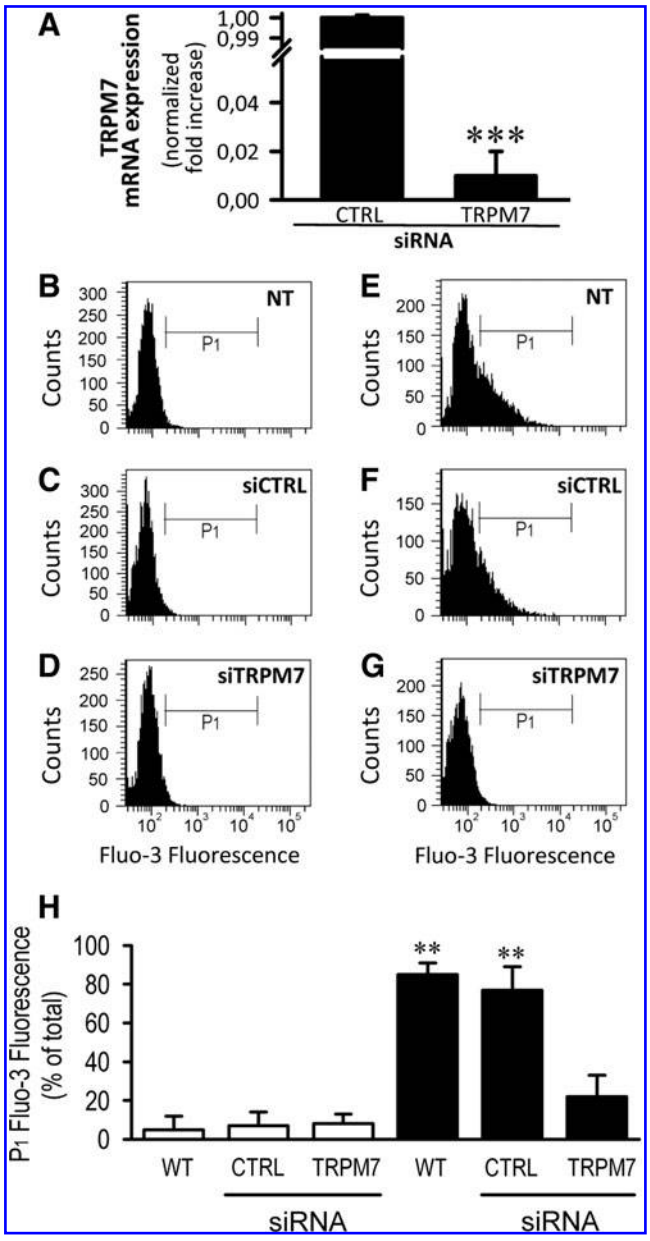

FIG. 7. Small interference RNA (siRNA) against TRPM7 protects neurons from LPS-induced Ca^{2+} overload. (A) Determination of the efficiency of the siRNA against TRPM7 (TRPM7) by quantitative PCR. Measurements were conducted in PC12 cells in triplicate, and values were normalized to GADPH mRNA expression and are relative to cells transfected with control siRNA (CTRL). Statistical differences were assessed by Student's *t*-test (Mann–Whitney). ***$p < 0.001$. Graphs show the mean ± SD ($n = 3$). Representative Fluo-3 **(B-G)** fluorescence histograms from separate experiments of differentiated PC12 neurons in the absence **(B–D)** or presence **(E–G)** of 20 μg/ml LPS for 48 h in NT **(B, E)**, siRNA control (siCTRL) transfected **(C, F)**, or siRNA against TRPM7 (siTRPM7) transfected cells **(D, G)**. Data obtained from experiments such as those depicted in the histograms above are summarized in **(H)**, showing cells in absence (open bars) or presence (closed bars) of LPS. Statistical differences were assessed by one-way ANOVA (Kruskal–Wallis) followed by Dunns *post hoc* test. **$p < 0.01$ relative to 0 μg/ml LPS. Graphs show the percentage (mean ± SD) of cells within the P_1 population of Fluo-3 ($n = 4$).

RNA inhibition of TRPM7 expression in neurons reduced LPS-induced Ca^{2+} influx

Due to the lack of specific pharmacological tools available to block TRPM7 channels, we used a small interference RNA (siRNA) to knockdown TRPM7 expression. For this purpose, PC12 neurons were transfected with siRNA against TRPM7 (siTRPM7). Considering that the efficiency of transfection in neurons is generally low, we transfected a red-labeled siRNA that acted as a reporter, which allowed for isolation of transfected cells through sorting. The knockdown efficiency was evaluated by qPCR only in the transfected cells sorted by fluorescence-activated cell sorter (FACS). As shown in Figure 7A, TRPM7 expression was reduced by ~99% compared with cells transfected with control siRNA (siCTRL). To study whether TRPM7 was involved in the LPS-induced calcium influx, differentiated PC12 neurons were transfected with siTRPM7 or siCTRL. Then, transfected cells were exposed to LPS and calcium levels were measured by flow cytometry with the calcium-sensitive probe Fluo-3. We transfected a red-labeled siRNA as a reporter to identify transfected cells. Thus, analysis of the experiments was performed in the transfected population only. Nontransfected (NT) cells and cells transfected with siCTRL showed an increase in Fluo-3 fluorescence when exposed to LPS (Fig. 7B, C and E, F). However, cells transfected with siTRPM7 failed to increase fluorescence when LPS was present (Fig. 7D, G), suggesting that TRPM7 is involved in the LPS-induced calcium influx. The experiments shown in Figure 7B–G are summarized in Figure 7H.

SiRNA inhibition of TRPM7 expression in neurons reduced LPS-induced cell death

We reasoned that if TRPM7 plays a role in LPS-induced cell death, it is expected that TRPM7 siRNA-transfected PC12 differentiated neurons should be resistant to LPS. Therefore, we assessed cell death by scoring Hoechst staining of chromatin-condensed cells and the cell morphology of each transfected cell. As shown in Figure 8A and 8B, siCTRL-transfected cells exposed to LPS showed an increase in chromatin condensation (arrowheads) and an aberrant cellular morphology when compared with LPS-treated siTRPM7-transfected cells, in which cell morphology was preserved (arrows indicate typical neuronal processes) (Fig. 8C, D). When several experiments were pooled, it became evident that LPS-induced cell death was significantly reduced in siTRPM7-transfected cells as compared with siCTRL cells or NT cells, but was not significantly different from cell death detected in nontreated siTRPM7-transfected cells (Fig. 8E).

To confirm the significance of TRPM7 involvement in LPS-induced cell death in neurons, we used HPN cultures enriched in neurons over glia. To evaluate the participation of TRPM7 in LPS-induced cell death in HPNs, cells were transfected with either siCTRL or siTRPM7, and cell death was evaluated. Neuronal cell death was significantly reduced in neurons that were transfected with siTRPM7 (Fig. 9C, D) compared with NT or siCTRL-transfected neurons (Fig. 9A, B) and was not significantly different from that in nontreated siRNA-TRPM7-transfected primary neurons (Fig. 9E).

Hoechst staining indicated that LPS-induced neuron death was apoptotic; so to address this point using a different approach, we conducted experiments to evaluate annexin V-FITC incorporation in PC12 neurons using flow cytometry.

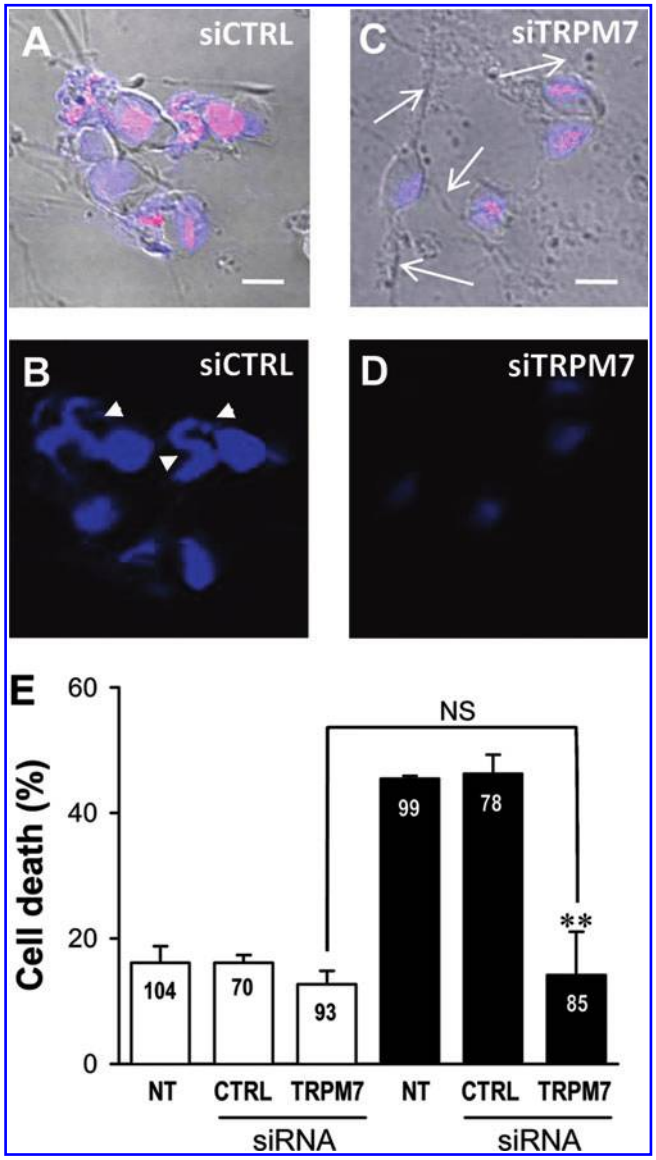

FIG. 8. siRNA against TRPM7 protects neurons from LPS-induced cell death. (A–D) Representative images of phase-contrast and Hoechst staining from experiments with neurons that were transfected with control siRNA (siCTRL) or with siRNA against TRPM7 (siTRPM7) and then exposed to 20 μg/ml LPS for 48 h. Hoechst staining alone is shown in **(B)** and **(D)**. Transfected neurons were identified by cotransfection with the red siRNA marker (red spots in cells). *Arrows* indicate typical neuronal processes. *Arrowheads* depict increases in chromatin condensation. Scale bar: 15 μm. Cells shown were fixed and mounted. **(E)** Cell death quantification in nontransfected neurons (NT) or transfected with control siRNA (CTRL) or with siRNA against TRPM7 (TRPM7) in the presence (filled bars) or absence (empty bars) of LPS, obtained from independent experiments such as those depicted in **(A–D)**. Values represent the percentage of the cells with nuclear chromatin condensation detected using Hoechst in either nontreated or transfected cells (red). Graph bars show the mean ± SD ($n = 3$). Six to 10 random areas/experiment were assessed. Numbers in bars denotes the total number of cells assessed in each condition. Statistical differences were assessed by one-way ANOVA (Kruskal–Wallis) followed by Dunns *post hoc* test. $^{**}p < 0.01$ against NT cells or CTRL cells in the presence of LPS. NS, nonsignificant. (To see this illustration in color the reader is referred to the web version of this article at www.liebertonline.com/ars).

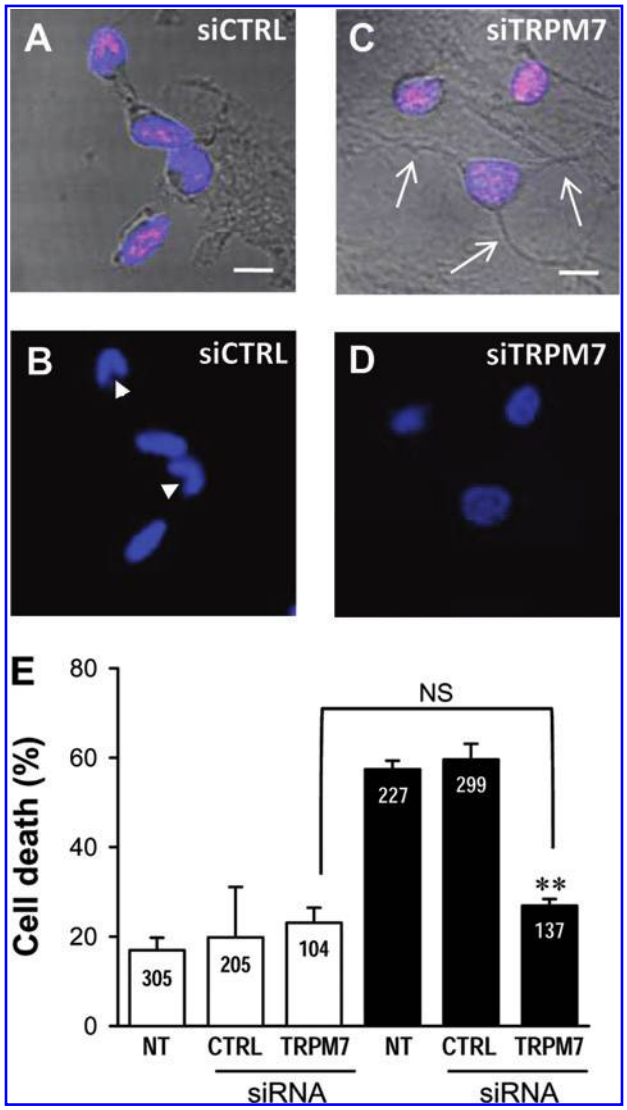

FIG. 9. siRNA against TRPM7 protects primary neurons from LPS-induced cell death. (A–D) Representative images of phase-contrast and Hoechst staining from experiments of primary neurons exposed to 20 μg/ml LPS for 48 h that were transfected with control siRNA (siCTRL) or with siRNA against TRPM7 (siTRPM7). Hoechst staining alone is shown in **(B** and **D)**. Transfected primary neurons were identified by cotransfection with the red siRNA marker (red spots in cells). *Arrows* indicate typical neuronal processes. *Arrowheads* depict increases in chromatin condensation. Scale bar: 15 μm. Cells shown were fixed and mounted. **(E)** Cell death quantification in primary neurons that were not transfected (NT), transfected with control siRNA (CTRL), or with siRNA against TRPM7 (siTRPM7) in the presence (filled bars) or absence (empty bars) of LPS. Cells were obtained from independent experiments such as those depicted in **(B–E)**. Values represent the percentage of cells with nuclear chromatin condensation detected using Hoechst in either NT or transfected cells (red). Graph bars show the mean ± SD ($N = 3$). Six to 10 random areas/experiment were assessed. Numbers in bars denotes the total number of cells assessed in each condition. Statistical differences were assessed by one-way ANOVA (Kruskal–Wallis) followed by Dunns *post hoc* test. $^{**}p < 0.01$ compared with NT cells or CTRL cells in the presence of LPS. NS, nonsignificant. (To see this illustration in color the reader is referred to the web version of this article at www.liebertonline.com/ars).

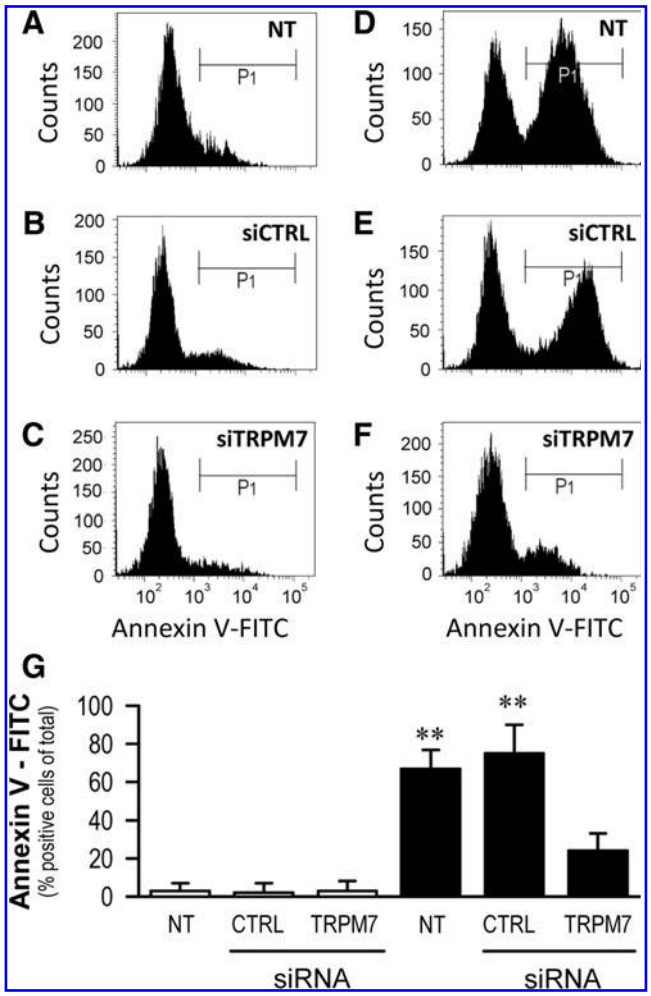

FIG. 10. siRNA against TRPM7 protects neurons from LPS-induced apoptotic cell death. Representative annexin V-FITC fluorescence histograms **(A–F)** from separate experiments of differentiated PC12 neurons cultured in the absence **(A–C)** or presence **(D–F)** of 20 μg/ml LPS for 48 h after being either NT **(A, D)**, transfected with siRNA control (siCTRL) **(B, E)**, or transfected with siRNA against TRPM7 (siTRPM7) **(C, F)**. Data obtained from experiments such as those depicted in the histograms above are summarized in **(G)**, showing cells in absence (open bars) or presence (closed bars) of LPS. Statistical differences were assessed by one-way ANOVA (Kruskal–Wallis) followed by Dunns *post hoc* test. $^{**}p < 0.01$ against 0 μg/ml LPS. Graph bars show the percentage (mean ± SD) of cells within the P_1 population of annexin V-FITC ($N = 4$).

As shown in Figure 10, NT cells and cells transfected with siCTRL showed an increase in annexin V-FITC fluorescence when exposed to LPS (Fig. 10A, B compared with D, E). However, cells transfected with siTRPM7 failed to increase in fluorescence when LPS was present (Fig. 10C compared with 10F), suggesting that TRPM7 was involved in LPS-induced neuronal death. Note that only transfected cells were evaluated. The experiments shown in Figure 10A–F are summarized in Figure 10E.

Next, we studied annexin V-FITC incorporation in HPNs using microscopy. To obtain a more pure HPN culture than the one used in the Hoechst staining experiments, we used a different protocol, achieving a culture containing over 90% of

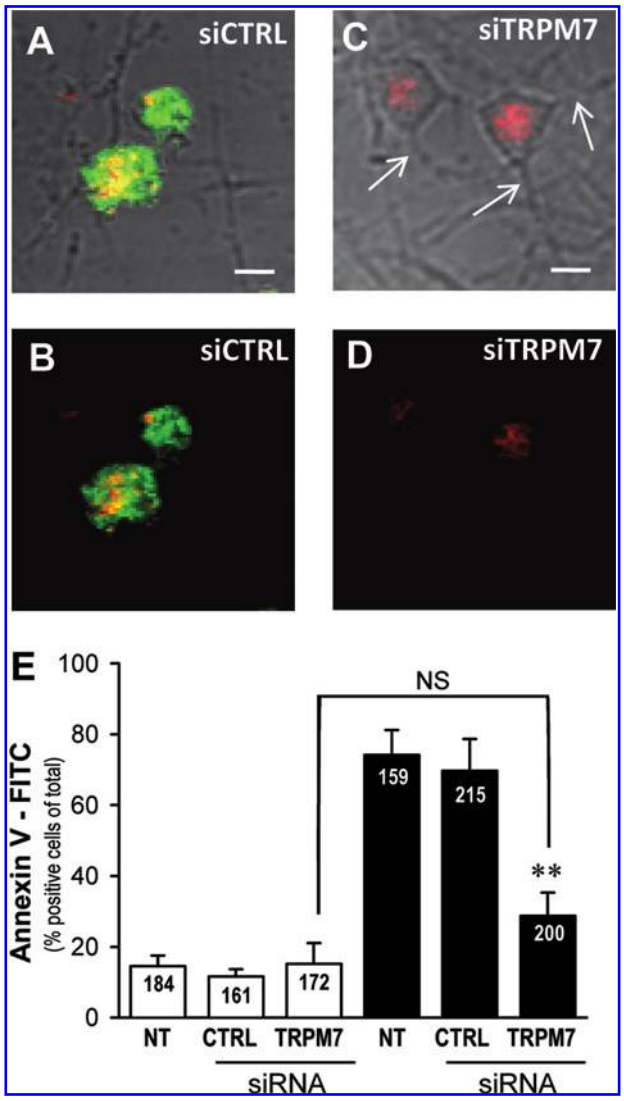

FIG. 11. siRNA against TRPM7 protects primary neurons from LPS-induced apoptotic cell death. (A–D) Representative images of phase-contrast and annexin V-FITC incorporation from experiments of HPNs exposed to 20 μg/ml LPS for 48 h after transfection with control siRNA (siCTRL) **(A, B)** or with siRNA against TRPM7 (siTRPM7) **(C, D)**. Transfected HPNs were identified by cotransfection with the red siRNA marker (red spots in cells). *Arrows* indicate typical neuronal processes. *Arrowheads* depict increases in chromatin condensation. Scale bar: 15 μm. Cells shown were fixed and mounted. **(E)** Cell death quantification as determined by annexin V-FITC positive cells in HPNs that were not transfected (NT), transfected with siCTRL, or transfected with siTRPM7 in the presence (filled bars) or absence (empty bars) of LPS, obtained from independent experiments such as those depicted in **(A–D)**. Values represent the percentage of annexin V-FITC positive cells of total cells (green) in either NT or transfected cells (red). Graphs show the mean ± SD ($n = 3$). Six to 10 random areas/experiment were assessed. Numbers in bars denote the total number of cells assessed in each condition. Statistical differences were assessed by one-way ANOVA (Kruskal–Wallis) followed by Dunns *post hoc* test. **: $p < 0.01$ compared with NT cells or CTRL cells in the presence of LPS. NS, nonsignificant. (To see this illustration in color, the reader is referred to the web version of this article at www.liebertonline.com/ars).

neurons. Similar to the Hoechst staining experiments, we examined only transfected cells indicated by the siRNA reporter (red). HPNs exposed to LPS showed a significant increase in neuronal cell death as measured by annexin V-FITC fluorescence (Fig. 11E, NT [empty bars compared with filled bars]), confirming the results obtained in differentiated PC12 neurons (Fig. 10). Next, HPNs were transfected with either siCTRL or siTRPM7, and cell death was evaluated. In these experiments, we observed that cell death was significantly increased in neurons which were transfected with siCTRL (Fig. 11A, B, E), as indicated by double positive staining for both red (siRNA reporter) and green (annexin V-FITC) and evident cell damage. However, HPNs transfected with siTRPM7 were resistant to LPS-induced detriment, showing only red labeling without green staining (Fig. 11C–E).

Discussion

Our data show that LPS is able to induce neuronal cell death in the absence of glial cells. Previous work has suggested that neuronal cell death observed after LPS exposure was related mainly to the activation of glial-related cells (40); however, since our experiments were conducted in a pure neuronal cell line (PC12 cells), the participation of other cell types in the process is not likely. In this scenario, the cell death seen in PC12 neurons after LPS exposure should be mediated in a cell-autonomous mechanism. Indeed, differentiated PC12 neurons express the LPS receptor, TLR-4, at the mRNA and protein levels, confirming that TLR-4 is expressed in neurons as has been reported by several independent groups (4, 36, 43, 57, 58, 62). In agreement with our data, it also has been reported that LPS can induce neuronal cell death directly (4, 25, 65). However, the mechanism involved in LPS-induced neuronal cell death has not been defined. It has been reported that exposure to LPS induces an increase in oxidative stress (18, 41, 51). This is also the case in our cell model, where an increase in overall ROS and, particularly, superoxide anions was detected after LPS exposure. Further, PKC, PLC, and PI3-K are involved in LPS-induced neuronal death, possibly as NAD(P)H oxidase activators rather than *via* effects on cell proliferation or apoptotic cell death. Our data show that DPI and apocynin exhibit an inhibitory effect, thus suggesting NAD(P)H oxidase participation. Nevertheless, caution should be taken, because DPI is a generic flavoprotein inhibitor, and recent data show that apocynin may act as a ROS scavenger instead of an NAD(P)H oxidase inhibitor in vascular cells (17).

Although ROS by itself is sufficient to alter cellular homeostasis and may explain the cell death phenotype observed (16, 23), in light of ample evidence showing that intracellular ROS has a number of effects on cellular physiology as well (10), we attempted to further define the mechanism involved in this process. The cell death process requires the activity of specific ion channels implicated in cell volume regulation and calcium homeostasis. Mounting evidence shows that a number of ion channels activities are modulated by ROS and participate in different cell death processes (15). Interestingly, in many cases, the inhibition of the activity of these ion channels protects against ROS-induced cell death, suggesting that ROS alone is not ultimately responsible for the process (9, 14, 15, 52).

Our data show that PC12 neurons display an altered calcium homeostasis, evidenced as a calcium overload, in response to LPS, suggesting the participation of calcium channels in our experimental model. Most cells exhibit ion channel activity, which is broadly defined as nonselective cation conductances (15), and many of these channels are activated by ROS. Our data show that generic inhibitors of these channels are able to reduce the effect of LPS on neuron viability. These data are in agreement with that obtained from other models, such as hepatocyte cell lines, in which blocking NSCC activity protects against ROS-induced cell death (5). Many of these NSCC activities have been identified at the genomic level, and a number of them belong to the TRP protein superfamily (13, 37, 60). Many of the TRP protein ion channels activities are positively modulated by ROS (15), but also it has been shown that ROS modulate these proteins at the gene expression level as has been shown for other genes (12, 22, 26, 44, 47, 50, 55). To explore this possibility, we identified candidate TRP channels that are modulated by ROS, involved in cell death, and able to permeate calcium or modulate calcium homeostasis. Therefore, we evaluated the expression of the TRPM4, TRPM2, and TRPM7 members of the TRP family after LPS exposure and found a significant increase in the expression of TRPM7. A large amount of evidence supports the idea that TRPM7 is linked to oxidative stress-induced neuron injury (1, 35, 56), and since TRPM7 channels have nonselective conductance of Ca^{2+} and Mg^{2+} (39, 45), they could be responsible for the calcium overload observed in our model. Thus, we would expect a significant increase in TRPM7 current triggered by LPS. Further experiments are necessary to elucidate this possibility.

Our data also show that LPS-induced TRPM7 overexpression is TLR4-dependent ROS production and is also mimicked by ROS exposure. Previous work has shown that TRPM7 expression can be increased by oxidative stress in monocytes (63) and by hypoxia-reperfusion in hippocampal neurons (21). Since hypoxia-reperfusion may produce ROS in the reperfusion step, it is likely that ROS are also the mechanism underlying TRPM7 overexpression in this model. To further study whether TRPM7 overexpression was necessary for LPS-induced neurotoxicity, we assessed cell death in PC12 and hippocampal neurons where TRPM7 expression has been knocked down with an siRNA. These experiments showed that TRPM7 overexpression is necessary for the effect of LPS in neuronal cell death.

In conclusion, our data establish ROS and TRPM7 as mediators of neuronal cell death and show that this pathway plays a critical role in LPS-induced neuronal death. These findings could serve as a basis for the development of novel neuroprotective agents for the treatment of sepsis and possibly other neurodegenerative disorders in which alterations in cellular Ca^{2+} homeostasis constitute a key pathophysiological factor.

Materials and Methods

PC12 cell culture

Rat pheochromocytoma PC12 cells (from American Type Culture Collection) were cultured in Dulbecco's modified Eagle's medium (DMEM) supplemented with heat-inactivated 10% horse serum, 5% fetal bovine serum (FBS), 50 units/ml penicillin, and 100 mg/ml streptomycin (Invitrogen). Differentiated PC12 neurons were obtained by plating cells into poly-L-lysine-coated dishes in the presence of 50 ng/ml NGF (Sigma-Aldrich) for a period of 5 days in DMEM

supplemented with 1% heat-inactivated horse serum and 1% FBS. The differentiation process was determined as described in Supplementary Figure S1 (Supplementary Data are available online at www.liebertonline.com/ars).

Primary neuronal culture

Primary neuronal cultures were obtained from neonate brains of Sprague-Dawley rats (1–3 days old or ≤24 h old) following institutionally approved procedures. Hippocampi were dissected in ice-cold Hank's buffer from neonate brains, and the collected tissue was incubated in 1.25% trypsin for 10 min at 37°C. Trypsin was deactivated by adding 10% bovine serum in minimum essential medium (MEM). The tissue was mechanically dissociated in MEM plus 10% FBS immediately through a fire-polished Pasteur pipette. A neuronal fraction was obtained by centrifugation of the dissociated brain cells in a density gradient prepared with Optiprep® and neurobasal medium supplemented with B27 (Neurobasal/B27) (Invitrogen), according to the instructions described by Brewer and Torricelli (6). The neuronal fraction was collected, washed twice with Neurobasal/B27, then plated on poly-L-lysine (Sigma-Aldrich) coated coverslips, and maintained at 37°C in a humidified atmosphere with 5% CO_2/95% air. Hippocampi collected from rats ≤24 h old were also treated with 5 μM of an equimolar mixture of uridine bioreagent (Sigma-Aldrich) and 5-fluoro-2′-deoxyuridine (Sigma-Aldrich) to suppress the growth of glial cells. Both procedures allowed us to obtain highly enriched neuronal cultures while avoiding the use of the antimitotic agent arabinoside cytosine and the concomitant culture toxicity reported by Ahlemeyer and Baumgart-Vogt (2). To quantify the neuronal enrichment provided by this procedure, neurons were immunodetected with an antibody directed against the microtubule-associated proteins 2 A and B (anti-MAP2A/2B; Millipore), and glial cells were visualized simultaneously using an antibody against the glial fibrillary acidic protein (anti-GFAP; Dako). Under standard culture conditions, the neuron/astrocyte ratio was less than 1:1 (2300 counted cells), whereas density gradient separation rendered a ratio that was increased ~70% (~3:1) or >90% (>10:1) for hippocampi from rats 1–3 days old or 24 h old, respectively (Supplementary Fig. S2).

Cell death determination

MTT assay and LDH release. After the treatments had been performed, cells were coincubated with anhydrous MTT (0.5 mg/ml) for 4 h and then solubilized with an isopropanol/DMSO solution. The optical density value was measured at 540 nm. Data were expressed as percentage of cell death. LDH release was defined as the ratio of LDH activity in the medium to LDH activity observed after total cell death, according to the manufacturer's protocol (Roche Boehringer-Mannheim) and was expressed as a percentage of total LDH release.

Hoechst staining and annexin V-FITC incorporation. After LPS treatment, cells were incubated with Hoechst 33342 (Molecular probes, Invitrogen) or annexin V-FITC (BD Pharmingen™) according to the manufacturer's protocol. Then cells were washed twice with phosphate-buffered saline (PBS) and fixed using PFA (3.7%) for 15 min at room temperature. Fixed cells were mounted and visualized with a confocal microscope (Olympus). Transfected cells were identified by red labeling (red-labeled siRNA).

In Hoechst staining experiments, both healthy and dead cells showed double labeling from the transfection indicator (red) and Hoechst stain (blue); however, dead cells showed blue nuclear spots (condensed chromatin) whereas healthy cells did not. The cell death score (Hoechst-positive cells/total) was determined by counting only the transfected cells and determining how many of them were Hoechst-positive (with condensed chromatin present).

In annexin V-FITC incorporation experiments by microscopy, dead cells exhibited green and red (siRNA reporter) labeling, whereas healthy cells showed a red mark only. The cell death score (annexin V-FITC-positive cells/total) was determined by counting only the transfected cells and determining how many of them were green (annexin V-FITC-positive).

In annexin V-FITC incorporation experiments by flow cytometry, after LPS treatment, cells were harvested with trypsin/EDTA, washed twice in ice-cold PBS, resuspended in annexin V-FITC, and incubated for 15–30 min at room temperature in the dark. Then, cells were analyzed immediately using flow cytometry (FACSCanto; BD Biosciences). Cells were cotransfected with $siRNA^{TRPM7}$ and $siRNA^{red}$ as a reporter. Then, annexin V-FITC incorporation was measured in the FL-1 channel (~483 nm), whereas fluorescence from the siRNA reporter (siRNA-red) was simultaneously detected in the FL-3 channel (>545 nm). Using the FACSDiva software, a population of red-positive cells (transfected cells) was defined, these cells were analyzed for annexin V-FITC incorporation. A minimum of 10,000 cells/sample were analyzed. Cellular dye intensity analysis was performed using FACSDiva software v4.1.1 (BD Biosciences).

qPCR and retrotranscriptase-PCR

Assays were run using a Rotor-gene system instrument (Corbet Research). Total RNA was extracted with TRIzol (Invitrogen) according to the manufacturer's protocol. DNAse I-treated RNA was used for reverse transcription with the Super Script II Kit (Invitrogen). Equal amounts of RNA were used as templates in each reaction. qPCR was performed using SYBR Green PCR Master Mix (AB Applied Biosystems). Data are presented as relative mRNA levels of the gene of interest normalized to relative GADPH mRNA levels. Primer sequence and PCR conditions are provided in the Supplementary Data. Total RNA obtained from rat brains was used as a positive control (PC) for TRPM7. As negative controls, reactions were also conducted using samples devoid of template. The amplified products were separated on a 2% agarose gel, which was subsequently stained with ethidium bromide (Sigma-Aldrich) and photographed under UV illumination. Images were acquired with a digital camera.

Western blot

Cells exposed to LPS were lysed, and protein extracts were subjected to 10% SDS-PAGE. Resolved proteins were transferred to a nitrocellulose membrane and blocked using 5% nonfat milk in TBS-T 1% at pH 7.4. Then, membranes were incubated first with goat anti-TRPM7 antibody (Abcam), washed, and then incubated with a horseradish peroxidase-conjugated rabbit anti-goat IgG secondary antibody (Abcam).

Peroxidase activity was detected through enhanced chemiluminescence (Sigma-Aldrich). TRPM7 protein content was determined by densitometric scanning of immunoreactive bands, and intensity values were obtained by densitometry of individual bands compared with tubulin (Sigma). For TLR-4, a Santa Cruz antibody was used. All experiments were normalized against the vehicle-stimulated condition. Procedural details are provided in the Supplementary Data.

Measurement of ROS production and [Ca^{2+}] by flow cytometry

Differentiated PC12 cells were plated and treated with 20 μg/ml LPS for 48 h. Cells were harvested with trypsin/EDTA, washed twice in ice-cold PBS, resuspended, and loaded with the following cell permeant dyes: for ROS measurements, either 5 μM DCF or 10 μM DHE and for Ca^{2+} determination, either 5 μM Fluo-3 or 15 μM Fura-Red (all from Invitrogen) for 15–30 min at room temperature in the dark. The labeled cells were then analyzed immediately by flow cytometry (FACSCanto; BD Biosciences). Cells were co-transfected (with $siRNA^{TRPM7}$ and $siRNA^{red}$ as a reporter). Experiments were performed, and then intracellular calcium levels were measured using Fluo-3 dye, which is detected in the FL-1 channel ($\sim$483 nm); whereas fluorescence from the siRNA reporter (siRNA-red), which is detected in the FL-3 channel (>545 nm), was recorded simultaneously. Using the FACSDiva software, a population of red-positive cells (transfected cells) was defined, and calcium levels for this population were analyzed. A minimum of 10,000 cells/sample were analyzed. Cellular dye intensity analysis was performed using FACSDiva software v4.1.1 (BD Biosciences).

Small interfering RNA against TRPM7 and transfections

SiRNA against rat TRPM7 (siTRPM7) was purchased from Dharmacon, and the siRNA sequence is as follows: $siRNA^{TRPM7}$: 5′-GAGAAAAGAUCCUGCGACAUU-3′. Red siRNA ($siRNA^{Red}$) was used as a transfection indicator, and nontargeting siRNA was used as a control (Dharmacon). Briefly, PC12 cells were plated overnight in 24-well plates and then differentiated using 50 ng/ml NGF for 5 days. Two days after NGF addition, cells were transfected with 5 nM siRNA (at a ratio of siTRPM7:$siRNA^{Red}$ equal to 10:1) using Lipofectamine 2000 transfection reagent (Invitrogen) according to the manufacturer's protocol in serum-free medium for 6 h. Primary neurons were plated for 5 days and then transfected with 5 nM siRNA using Lipofectamine 2000 transfection reagent in serum-free medium for 6 h. Experiments were performed 3–4 days after transfection.

Reagents

LPS from *E. coli* was purchased from Sigma (0127:B8). Diphenyliodonium, Chelerythrine, U73122, and Ly424002 were purchased from Calbiochem. DTT, apocynin, and H_2O_2 were purchased from Sigma. Buffers and salts were purchased from Merck Biosciences (Darmstadt).

Data analysis

All results are presented as mean ± SD from three or more independent experiments. ANOVA followed by Bonferroni or Dunn's *post hoc* tests and Student's *t*-test were used. The significance level was set at $p < 0.05$.

Acknowledgments

This work was supported by grants UNAB-DI 33-11/R (F.S.), UNAB-DI 40-09/R (F.S.), Fondecyt 11080119 (F.S.), Mecesup UAB0802 (C.E.), Fondecyt 11080019 (D.V.), and Fondecyt 3090030 (O.P.). We are grateful to Walter Low and Marcela Hermoso for kindly providing the TLR-4 inhibitor TBX2. This work received institutional support from grant Fondecyt-FONDAP 15010006.

Author Disclosure Statement

No competing financial interests exist.

References

1. Aarts M, Iihara K, Wei WL, Xiong ZG, Arundine M, Cerwinski W, MacDonald JF, and Tymianski M. A key role for TRPM7 channels in anoxic neuronal death. *Cell* 115: 863–877, 2003.
2. Ahlemeyer B and Baumgart-Vogt E. Optimized protocols for the simultaneous preparation of primary neuronal cultures of the neocortex, hippocampus and cerebellum from individual newborn (P0.5) C57Bl/6J mice. *J Neurosci Methods* 149: 110–120, 2005.
3. Aracena-Parks P, Goonasekera SA, Gilman CP, Dirksen RT, Hidalgo C, and Hamilton SL. Identification of cysteines involved in S-nitrosylation, S-glutathionylation, and oxidation to disulfides in ryanodine receptor type 1. *J Biol Chem* 281: 40354–40368, 2006.
4. Arciszewski MB, Sand E, and Ekblad E. Vasoactive intestinal peptide rescues cultured rat myenteric neurons from lipopolysaccharide induced cell death. *Regul Pept* 146: 218–223, 2008.
5. Barros LF, Stutzin A, Calixto A, Catalan M, Castro J, Hetz C, and Hermosilla T. Nonselective cation channels as effectors of free radical-induced rat liver cell necrosis. *Hepatology* 33: 114–122, 2001.
6. Brewer GJ and Torricelli JR. Isolation and culture of adult neurons and neurospheres. *Nat Protoc 2*: 1490–1498, 2007.
7. Cheret C, Gervais A, Lelli A, Colin C, Amar L, Ravassard P, Mallet J, Cumano A, Krause KH, and Mallat M. Neurotoxic activation of microglia is promoted by a Nox1-dependent NADPH oxidase. *J Neurosci* 28: 12039–12051, 2008.
8. Clement HW, Vazquez JF, Sommer O, Heiser P, Morawietz H, Hopt U, Schulz E, and von DE. Lipopolysaccharide-induced radical formation in the striatum is abolished in Nox2 gp91phox-deficient mice. *J Neural Transm* 117: 13–22, 2010.
9. Coombes E, Jiang J, Chu XP, Inoue K, Seeds J, Branigan D, Simon RP, and Xiong ZG. Pathophysiological relevant levels of hydrogen peroxide induces glutamate-independent neurodegeneration that involves activation of TRPM7 channels. *Antioxid Redox Signal* 14: 1815–1827, 2011.
10. Droge W. Free radicals in the physiological control of cell function. *Physiol Rev* 82: 47–95, 2002.
11. Gayle DA, Ling Z, Tong C, Landers T, Lipton JW, and Carvey PM. Lipopolysaccharide (LPS)-induced dopamine cell loss in culture: roles of tumor necrosis factor-alpha, interleukin-1beta, and nitric oxide. *Brain Res Dev* 133: 27–35, 2002.
12. Goyal P, Weissmann N, Grimminger F, Hegel C, Bader L, Rose F, Fink L, Ghofrani HA, Schermuly RT, Schmidt HH,

Seeger W, and Hanze J. Upregulation of NAD(P)H oxidase 1 in hypoxia activates hypoxia-inducible factor 1 via increase in reactive oxygen species. *Free Radic Biol Med* 36: 1279–1288, 2004.
13. Harteneck C, Plant TD, and Schultz G. From worm to man: three subfamilies of TRP channels. *Trends Neurosci* 23: 159–166, 2000.
14. Hecquet CM, Ahmmed GU, Vogel SM, and Malik AB. Role of TRPM2 channel in mediating H_2O_2-induced Ca^{2+} entry and endothelial hyperpermeability. *Circ Res* 102: 347–355, 2008.
15. Henriquez M, Armisen R, Stutzin A, and Quest AF. Cell death by necrosis, a regulated way to go. *Curr Mol Med* 8: 187–206, 2008.
16. Hidalgo C and Carrasco MA. Redox control of brain calcium in health and disease. *Antioxid Redox Signal* 14: 1203–1207, 2010.
17. Heumüller S, Wind S, Barbosa-Sicard E, Schmidt HHHW, Schröder K, and Brandes RP. Apocynin is not an inhibitor of vascular NADPH oxidases but an antioxidant. *Hypertension* 51: 211–217, 2008.
18. Imaizumi T, Itaya H, Fujita K, Kudoh D, Kudoh S, Mori K, Fujimoto K, Matsumiya T, Yoshida H, and Satoh K. Expression of tumor necrosis factor-alpha in cultured human endothelial cells stimulated with lipopolysaccharide or interleukin-1alpha. *Arterioscler Thromb Vasc Biol* 20: 410–415, 2000.
19. Impellizzeri D, Esposito E, Mazzon E, Paterniti I, Di PR, Bramanti P, and Cuzzocrea S. Effect of apocynin, a NADPH oxidase inhibitor, on acute lung inflammation. *Biochem Pharmacol* 81: 636–648, 2011.
20. Inoue K, Branigan D, and Xiong ZG. Zinc-induced neurotoxicity mediated by transient receptor potential melastatin 7 channels. *J Biol Chem* 285: 7430–7439, 2010.
21. Jiang H, Tian SL, Zeng Y, Li LL, and Shi J. TrkA pathway(s) is involved in regulation of TRPM7 expression in hippocampal neurons subjected to ischemic-reperfusion and oxygen-glucose deprivation. *Brain Res Bull* 76: 124–130, 2008.
22. Kiritoshi S, Nishikawa T, Sonoda K, Kukidome D, Senokuchi T, Matsuo T, Matsumura T, Tokunaga H, Brownlee M, and Araki E. Reactive oxygen species from mitochondria induce cyclooxygenase-2 gene expression in human mesangial cells: potential role in diabetic nephropathy. *Diabetes* 52: 2570–2577, 2003.
23. Koutsilieri E, Scheller C, Tribl F, and Riederer P. Degeneration of neuronal cells due to oxidative stress; microglial contribution. *Parkinsonism Relat Disord* 8: 401–406, 2002.
24. Kunsch C and Medford RM. Oxidative stress as a regulator of gene expression in the vasculature. *Circ Res* 85: 753–766, 1999.
25. Li B, Guo YS, Sun MM, Dong H, Wu SY, Wu DX, and Li CY. The NADPH oxidase is involved in lipopolysaccharide-mediated motor neuron injury. *Brain Res* 1226: 199–208, 2008.
26. Li DW and Spector A. Hydrogen peroxide-induced expression of the proto-oncogenes, c-jun, c-fos and c-myc in rabbit lens epithelial cells. *Mol Cell Biochem* 173: 59–69, 1997.
27. Lopes LR, Hoyal CR, Knaus UG, and Babior BM. Activation of the leukocyte NADPH oxidase by protein kinase C in a partially recombinant cell-free system. *J Biol Chem* 274: 15533–15537, 1999.
28. Low W, Mortlock A, Petrovska L, Dottorini T, Dougan G, and Crisanti A. Functional cell permeable motifs within medically relevant proteins. *J Biotechnol* 129: 555–564, 2007.
29. Lu CH, Chang WN, Chuang YC, and Chang HW. Gram-negative bacillary meningitis in adult post-neurosurgical patients. *Surg Neurol* 52: 438–443, 1999.
30. Lustig S, Danenberg HD, Kafri Y, Kobiler D, and Ben--Nathan D. Viral neuroinvasion and encephalitis induced by lipopolysaccharide and its mediators. *J Exp Med* 176: 707–712, 1992.
31. Mangi RJ, Quintiliani R, and Andriole VT. Gram-negative bacillary meningitis. *Am J Med* 59: 829–836, 1975.
32. Mates JM, Segura JA, Alonso FJ, and Marquez J. Intracellular redox status and oxidative stress: implications for cell proliferation, apoptosis, and carcinogenesis. *Arch Toxicol* 82: 273–299, 2008.
33. Matkar SS, Wrischnik LA, and Hellmann-Blumberg U. Production of hydrogen peroxide and redox cycling can explain how sanguinarine and chelerythrine induce rapid apoptosis. *Arch Biochem Biophys* 477: 43–52, 2008.
34. Mayhan WG. Effect of lipopolysaccharide on the permeability and reactivity of the cerebral microcirculation: role of inducible nitric oxide synthase. *Brain Res* 792: 353–357, 1998.
35. Miller BA. The role of TRP channels in oxidative stress-induced cell death. *J Membr Biol* 209: 31–41, 2006.
36. Mishra BB, Mishra PK, and Teale JM. Expression and distribution of Toll-like receptors in the brain during murine neurocysticercosis. *J Neuroimmunol* 181: 46–56, 2006.
37. Montell C. The TRP superfamily of cation channels. *Sci STKE* 2005: re3, 2005.
38. Morgan MJ, Kim YS, and Liu ZG. TNFalpha and reactive oxygen species in necrotic cell death. *Cell Res* 18: 343–349, 2008.
39. Nadler MJ, Hermosura MC, Inabe K, Perraud AL, Zhu Q, Stokes AJ, Kurosaki T, Kinet JP, Penner R, Scharenberg AM, and Fleig A. LTRPC7 is a Mg.ATP-regulated divalent cation channel required for cell viability. *Nature* 411: 590–595, 2001.
40. Olson JK and Miller SD. Microglia initiate central nervous system innate and adaptive immune responses through multiple TLRs. *J Immunol* 173: 3916–3924, 2004.
41. Park HS, Chun JN, Jung HY, Choi C, and Bae YS. Role of NADPH oxidase 4 in lipopolysaccharide-induced proinflammatory responses by human aortic endothelial cells. *Cardiovasc Res* 72: 447–455, 2006.
42. Paterniti I, Galuppo M, Mazzon E, Impellizzeri D, Esposito E, Bramanti P, and Cuzzocrea S. Protective effects of apocynin, an inhibitor of NADPH oxidase activity, in splanchnic artery occlusion and reperfusion. *J Leukoc Biol* 88: 993–1003, 2010.
43. Prehaud C, Megret F, Lafage M, and Lafon M. Virus infection switches TLR-3-positive human neurons to become strong producers of beta interferon. *J Virol* 79: 12893–12904, 2005.
44. Roebuck KA, Rahman A, Lakshminarayanan V, Janakidevi K, and Malik AB. H2O2 and tumor necrosis factor-alpha activate intercellular adhesion molecule 1 (ICAM-1) gene transcription through distinct cis-regulatory elements within the ICAM-1 promoter. *J Biol Chem* 270: 18966–18974, 1995.
45. Runnels LW, Yue L, and Clapham DE. TRP-PLIK, a bifunctional protein with kinase and ion channel activities. *Science* 291: 1043–1047, 2001.
46. Sanchez G, Pedrozo Z, Domenech RJ, Hidalgo C, and Donoso P. Tachycardia increases NADPH oxidase activity and RyR2 S-glutathionylation in ventricular muscle. *J Mol Cell Cardiol* 39: 982–991, 2005.
47. Schreck R, Rieber P, and Baeuerle PA. Reactive oxygen intermediates as apparently widely used messengers in the activation of the NF-kappa B transcription factor and HIV-1. *EMBO J* 10: 2247–2258, 1991.
48. Simard JM, Chen M, Tarasov KV, Bhatta S, Ivanova S, Melnitchenko L, Tsymbalyuk N, West GA, and Gerzanich V. Newly expressed SUR1-regulated NC(Ca-ATP) channel

mediates cerebral edema after ischemic stroke. *Nat Med* 12: 433–440, 2006.
49. Simard JM, Tsymbalyuk O, Ivanov A, Ivanova S, Bhatta S, Geng Z, Woo SK, and Gerzanich V. Endothelial sulfonylurea receptor 1-regulated NC Ca-ATP channels mediate progressive hemorrhagic necrosis following spinal cord injury. *J Clin Invest* 117: 2105–2113, 2007.
50. Simon AR, Rai U, Fanburg BL, and Cochran BH. Activation of the JAK-STAT pathway by reactive oxygen species. *Am J Physiol* 275: C1640–C1652, 1998.
51. Simon F and Fernandez R. Early lipopolysaccharide-induced reactive oxygen species production evokes necrotic cell death in human umbilical vein endothelial cells. *J Hypertens* 27: 1202–1216, 2009.
52. Simon F, Leiva-Salcedo E, Armisen R, Riveros A, Cerda O, Varela D, Eguiguren AL, Olivero P, and Stutzin A. Hydrogen peroxide removes TRPM4 current desensitization conferring increased vulnerability to necrotic cell death. *J Biol Chem* 285: 37150–37158, 2010.
53. Simon F and Stutzin A. Protein kinase C-mediated phosphorylation of $p47^{phox}$ modulates platelet-derived growth factor-induced H_2O_2 generation and cell proliferation in human umbilical vein endothelial cells. *Endothelium* 15: 175–188, 2008.
54. Simon F, Varela D, Eguiguren AL, Diaz LF, Sala F, and Stutzin A. Hydroxyl radical activation of a Ca^{2+}-sensitive nonselective cation channel involved in epithelial cell necrosis. *Am J Physiol Cell Physiol* 287: C963–C970, 2004.
55. Stauble B, Boscoboinik D, Tasinato A, and Azzi A. Modulation of activator protein-1 (AP-1) transcription factor and protein kinase C by hydrogen peroxide and D-alpha-tocopherol in vascular smooth muscle cells. *Eur J Biochem* 226: 393–402, 1994.
56. Sun HS, Jackson MF, Martin LJ, Jansen K, Teves L, Cui H, Kiyonaka S, Mori Y, Jones M, Forder JP, Golde TE, Orser BA, MacDonald JF, and Tymianski M. Suppression of hippocampal TRPM7 protein prevents delayed neuronal death in brain ischemia. *Nat Neurosci* 12: 1300–1307, 2009.
57. Tang SC, Arumugam TV, Xu X, Cheng A, Mughal MR, Jo DG, Lathia JD, Siler DA, Chigurupati S, Ouyang X, Magnus T, Camandola S, and Mattson MP. Pivotal role for neuronal Toll-like receptors in ischemic brain injury and functional deficits. *Proc Natl Acad Sci U S A* 104: 13798–13803, 2007.
58. Tang SC, Lathia JD, Selvaraj PK, Jo DG, Mughal MR, Cheng A, Siler DA, Markesbery WR, Arumugam TV, and Mattson MP. Toll-like receptor-4 mediates neuronal apoptosis induced by amyloid beta-peptide and the membrane lipid peroxidation product 4-hydroxynonenal. *Exp Neurol* 213: 114–121, 2008.
59. Varela D, Simon F, Riveros A, Jorgensen F, and Stutzin A. NAD(P)H oxidase-derived H_2O_2 signals chloride channel activation in cell volume regulation and cell proliferation. *J Biol Chem* 279: 13301–13304, 2004.
60. Venkatachalam K and Montell C. TRP channels. *Annu Rev Biochem* 76: 387–417, 2007.
61. Villaran RF, Espinosa-Oliva AM, Sarmiento M, de Pablos RM, Arguelles S, Delgado-Cortes MJ, Sobrino V, van RN, Venero JL, Herrera AJ, Cano J, and Machado A. Ulcerative colitis exacerbates LPS-induced damage to the nigral dopaminergic system: potential risk factor in Parkinson's disease. *J Neurochem* 114: 1687–1700, 2010.
62. Wadachi R and Hargreaves KM. Trigeminal nociceptors express TLR-4 and CD14: a mechanism for pain due to infection. *J Dent Res* 85: 49–53, 2006.
63. Wuensch T, Thilo F, Krueger K, Scholze A, Ristow M, and Tepel M. High glucose-induced oxidative stress increases transient receptor potential channel expression in human monocytes. *Diabetes* 59: 844–849, 2010.
64. Ximenes VF, Kanegae MP, Rissato SR, and Galhiane MS. The oxidation of apocynin catalyzed by myeloperoxidase: proposal for NADPH oxidase inhibition. *Arch Biochem Biophys* 457: 134–141, 2007.
65. Yeh SH, Hung JJ, Gean PW, and Chang WC. Hypoxia-inducible factor-1alpha protects cultured cortical neurons from lipopolysaccharide-induced cell death via regulation of NR1 expression. *J Neurosci* 28: 14259–14270, 2008.

Address correspondence to:
Dr. Felipe Simon
Departamento de Ciencias Biologicas
Facultad de Ciencias Biologicas & Facultad de Medicina
Universidad Andres Bello
Av. Republica 217
8370146 Santiago
Chile

E-mail: fsimon@unab.cl

Date of first submission to ARS Central, December 6, 2010; date of final revised submission, May 1, 2011; date of acceptance, May 3, 2011.

Abbreviations Used

AP-1 = activator protein-1
Apo = apocynin
DCF = dichlorodihydrofluorescein
DHE = diacetate dihydroethidium
DMEM = Dulbecco's modified Eagle's medium
DPI = diphenyleneiodonium sulfate
DTT = dithiothreitol
FACS = fluorescence-activated cell sorter
FBS = fetal bovine serum
H_2O_2 = hydrogen peroxide
HEK = human embryonic kidney
HIF-1 = hypoxia-inducible factor-1
HPN = hippocampal primary neuron
ICAM-1 = intercellular adhesion molecule-1
LDH = lactate dehydrogenase
LPS = lipopolysaccharide
MEM = minimum essential medium
MTT = 3-(4,5-dimethylthiazol-2-yl)-2,5-diphenyltetrazolium bromide
NGF = nerve growth factor
NSCC = nonselective cationic channel
PBS = phosphate-buffered saline
PI3-K = phosphoinositide 3-kinase
PKC = protein kinase C
PLC = phospholipase C
ROS = reactive oxygen species
siRNA = small interference RNA
TLR-4 = Toll-like receptor-4
TRP = transient receptor potential
TRPM7 = transient receptor potential melastatin 7
VCAM-1 = vascular cell adhesion molecule-1

This article has been cited by:

1. María Gabriela Morales, Yaneisi Vazquez, María José Acuña, Juan Carlos Rivera, Felipe Simon, José Diego Salas, Joel Álvarez Ruf, Enrique Brandan, Claudio Cabello-Verrugio. 2012. Angiotensin II-induced pro-fibrotic effects require p38MAPK activity and transforming growth factor beta 1 expression in skeletal muscle cells. *The International Journal of Biochemistry & Cell Biology* **44**:11, 1993-2002. [CrossRef]
2. Hsiang#Chin Chen, Li#Ting Su, Omayra González#Pagán, Jeffrey D. Overton, Loren W. Runnels. 2012. A key role for Mg 2+ in TRPM7's control of ROS levels during cell stress. *Biochemical Journal* **445**:3, 441-448. [CrossRef]